DYNAMICS AND CHAOS

RICKY LIN

Abstract. In this review, we will talk about chaos in nonlinear dynamical systems. First, we introduce what a dynamical system is with an emphasis on iterated maps and define important concepts like fixed points and bifurcation. Next, we will analyze the logistic map and its chaotic behavior under certain conditions. Finally, we define chaos and its necessary conditions and prove that the Hénon map fulfills the condition for chaos.

Contents

1. Dynamics

1.1. **Basic Definitions.** A **dynamical system** is a system wherein a function, which may depend on time, describes the evolution of a point/vector (called a **state**) in a geometric space. Assuming a deterministic world, there can only be one future state that follows from the current state after a given interval of time passes. There are two kinds of dynamical systems: differential equations, which describes how the system evolves or changes in continuous time, and **iterated maps** (or just **maps**), which take discrete time.

Date: June 2021.

This paper primarily focuses on maps since their discrete nature provides simpler examples of chaos. Maps have the form

$$x_{n+1} = f(x_n), \tag{1.1}$$

where $f : \mathbb{R} \to \mathbb{R}$ is a smooth function. If f is linear in x_n, then the map is called linear. Otherwise, it is **nonlinear**.

We will look at well-known nonlinear maps to study chaos. By choosing a starting state x_0 (called the **initial condition**), maps generate a sequence of states

$$x_0, x_1, x_2, \ldots \tag{1.2}$$

by substituting x_0 into f to get x_1, then x_1 into f to get x_2, and so on. Denote this sequence the **orbit** starting from x_0. We imagine the orbit as the path/trajectory the map takes after starting from a specific x_0. The plot of all possible orbits on the graph x_{n+1} vs x_n is called the **phase space**.

1.2. **Equilibrium and Stability.** In dynamics, we study the behavior of dynamical systems as they evolve over time. One important behavior we are concerned about is whether the system will reach some state and remain there forever. For a state x_f such that

$$f(x_f) = x_f, \tag{1.3}$$

we call x_f a(n) **fixed point/equilibrium**. Since $x_{f+1} = f(x_f) = x_f$, any orbit with $x_n = x_f$ will always remain at x_f for all future iterations.

However, what happens to a nearby orbit that is a small perturbation η_n away from a fixed point x_f? Let $x_n = x_f + \eta_n$. We want to see whether that perturbation increases or decreases as n increases. We have that:

$$\begin{aligned} x_f + \eta_{n+1} &= x_{n+1} \\ &= f(x_f + \eta_n) \\ &= f(x_f) + f'(x_f)\eta_n + O(\eta_n^2). \end{aligned} \tag{1.4}$$

Now using the fact that $f(x_f) = x_f$,

$$\eta_{n+1} = f'(x_f)\eta_n + O(\eta_n^2). \tag{1.5}$$

Then, we linearize the map by ignoring the $O(\eta_n^2)$ term and get $\eta_{n+1} = f'(x_f)\eta_n$, where we denote the eigenvalue as $\lambda = f'(x_f)\eta_n$. Thus, we can solve this map with a general formula:

$$\eta_n = \lambda^n \eta_0. \tag{1.6}$$

We see now that if $|\lambda| < 1$, then $\eta_n \to 0$ as $n \to \infty$. Intuitively, this says that any small perturbation from the fixed point gets smaller and smaller as we iterate the map. We call x_f a **stable fixed point**. If $|\lambda| > 1$, then we see that η_n continues to increase, so the orbit moves away the fixed point. We instead call x_f a **unstable fixed point**. In the **marginal** case where $|\lambda| = 1$, we cannot yet say anything and must consider the neglected $O(\eta_n^2)$ term to determine the stability. While we have used linearization to determine the local stability of the fixed point, this analysis extends to nonlinear maps as well.

A generalization of a fixed point is a periodic point. A **periodic point** is a state x_p such that

$$f_n(x_p) = x_p, \tag{1.7}$$

for some n, where f_n is the nth iteration of the map f. The smallest positive integer n such that (1.7) holds is called the **period** of x_p. We easily see that a fixed point is a periodic point with period one. In general, if the period is m, the orbit visits x_p every mth iteration. Using the same derivation for fixed points, we say that a periodic point is attracting if $|f_n'| < 1$ and repelling if $|f_n'| > 1$.

Stable fixed points and attracting periodic points are examples of **attractors**. We define an **attractor** A as a set of points in the phase space such that:

(1) If $a \in A$, then $f(a) \in A$ for any iterations
(2) There is a neighborhood of A called the **basin of attraction** with all the points that converges to A as $n \to \infty$
(3) There is no non-empty subset of A with the previous two properties

Essentially, an attractor is a subset of the phase space where within a neighborhood around it, all the orbits will approach the attractor. Unstable fixed points and repelling periodic points are examples of **repellers**, which are defined analogously to attractors, but the orbits are moving away from the set.

Attractors (and repellers) can have a variety of geometric shapes. A stable fixed point is an attractor where the set is just a point. In discrete-time, we can also have attractors as a finite number of attracting periodic points that are visited in sequence (we call this sequence a **periodic orbit**). We will see later on that chaos is tied to the shape of the attractor.

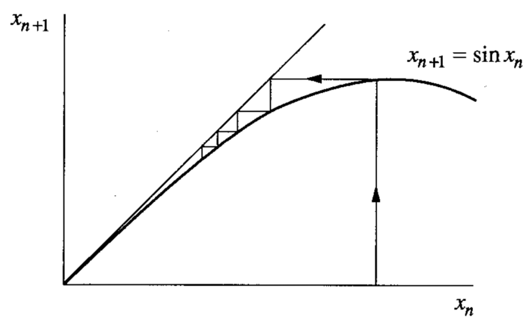

FIGURE 1. The map $x_{n+1} = \sin(x_n)$ has a marginal case, so use cobwebbing to determine stability. Reprinted from [1], p.352.

1.3. **Cobwebs.** To analyze some of the marginal cases where $|\lambda| = 1$, we introduce **cobwebs** as a visual technique to analyze the global behavior of maps. The picture is constructed like so: on phase space of x_{n+1} vs x_n, plot the functions

$$x_{n+1} = f(x_n), \quad \text{and} \quad x_{n+1} = x_n. \tag{1.8}$$

Now, for an initial condition x_0 on the horizontal axis, draw a vertical line upwards until it touches $f(x_0)$. The height of this vertical line is x_1. Then, to generate the line for x_2, instead of returning to the horizontal axis and drawing a vertical line from x_1, we instead draw a horizontal line from $f(x_0)$ until the line touches the diagonal $x_{n+1} = x_n$ (this intersection should lie directly above x_1). We now draw a vertical line upwards until it intersects f again, and its height is $x_2 - x_1$. We repeat this algorithm n times if we want to draw the first n states of an orbit. Figures 1 and 2 are two examples of cobwebs.

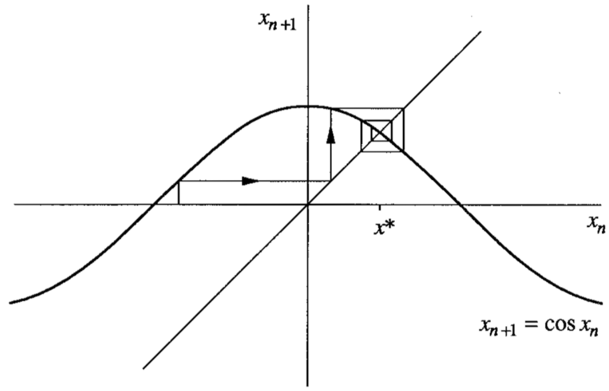

FIGURE 2. The map $x_{n+1} = \cos(x_n)$ displays a spiraling behavior towards the fixed point. Reprinted from [1], p.352.

To see how a cobweb can help us determine stability, we note that every vertical line after the first one represents the distance between two consecutive states in an orbit. If the length of these lines goes to zero, that means that the distance between two consecutive states goes to zero, and so the orbit from the initial condition x_0 converges to a limit x_∞. Thus, we have found a stable fixed point since the orbit starting from x_∞ will now remain at that value, and orbits starting nearby are getting close to this fixed point. In other words, we are graphically looking for the point where $f(x_n) = x_n$, which is the definition of a fixed point, and graphically analyzing the behavior of orbits close to it.

1.4. **Bifurcations.** Maps may depend on some control parameter r. This parameter is often a characteristic of the model the map represents (ex. varying weights on top of a beam). In studying such maps, we are interested in what happens their behavior as we alter r. Most notably, equilibrium points could be created, destroyed, or have their stability and/or value changed. We call such a transition a **bifurcation** and the value of r where a bifurcation occurs a **bifurcation point**. We depict these changes with what is called a **bifurcation diagram**, where we plot x vs r and only plot the equilibrium points on the graph. To distinguish between fixed points, we use bold lines for stable ones and dotted lines for unstable ones.

A **saddle-node bifurcation** creates and destroys fixed points. We start with one stable fixed point and one unstable fixed point. As we change r, the two fixed points move closer together until they collide when we reach the bifurcation point. Their collision creates a half-stable point, where orbits on the stable side approach the point while orbits on the unstable side are repelled. Then, changing r further results in the two fixed points annihilating each other. Similarly, we can run this in reverse and create two fixed points from seemingly nothing by altering r in the other direction. We show an example in Figure 3, and its bifurcation diagram in Figure 4 in continuous time for simplicity.

A **transcritical bifurcation** happens when a fixed point changes its stability as the parameter is changed. Consider two stable fixed points, one stable at the origin, and one unstable at $-r$. As we decrease positive r, the unstable fixed point approaches the stable fixed point until they form a half-stable fixed point at the

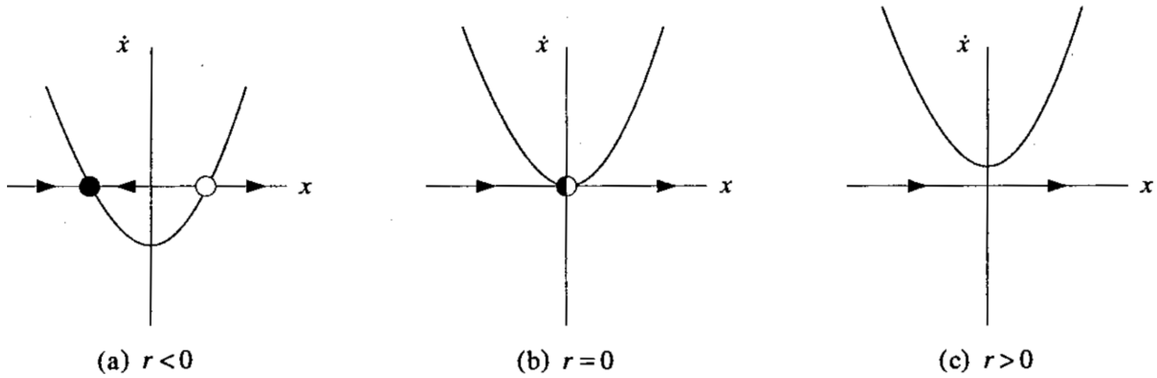

FIGURE 3. Example of a saddle-node bifurcation where the closed dot is a stable fixed point and the open dot is an unstable fixed point. Reprinted from [1], p.45.

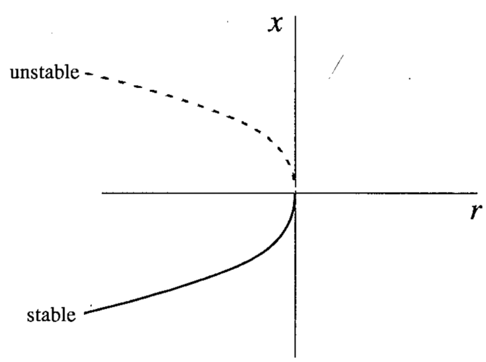

FIGURE 4. The previous figure's corresponding bifurcation diagram. Reprinted from [1], p.46.

bifurcation point $r = 0$. However, as we continue and take r negative, the unstable fixed point remains at the origin while the stable fixed point moves out along the positive x-axis. This is interpreted as the fixed points switching their stabilities.

A **pitchfork bifurcation** is a combination of fixed point creation/destruction and changing stability. There are two kinds of pitchfork bifurcation: supercritical and subcritical. A **supercritical pitchfork bifurcation** occurs when, as we vary r, a stable fixed point changes to an unstable one, and two new stable fixed points are created, one to each side of the now unstable fixed point. A **subcritical pitchfork bifurcation** occurs when, as we vary r, an unstable fixed point changes to a stable one, and two new unstable fixed points are created, one to each side of the now stable fixed point. A subcritical bifurcation produces the opposite stability as what occurs in the supercritical case.

A **period doubling bifurcation** occurs when a new periodic orbit is created from an existing periodic orbit, the newer one with double the period. Consider a periodic orbit that visits x_1, x_2 in sequence. It is clear that the orbit has period two, since the orbit oscillates between x_1 and x_2, each point with period two. A period doubling bifurcation creates a new periodic orbit that repeatedly visits x_1', x_2', x_3', x_4'

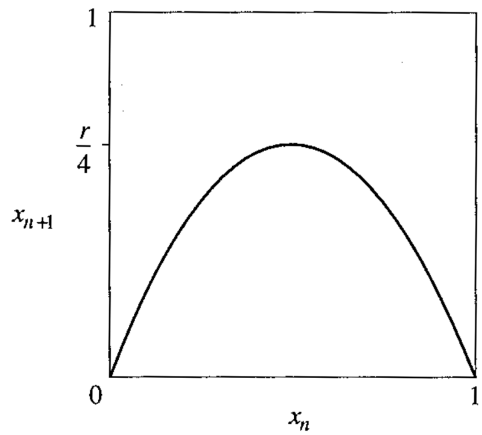

FIGURE 5. Logistic map. Reprinted from [1], p.353.

in sequence, thus doubling the period of the former orbit. We will show an example of this with the logistic map.

2. LOGISTIC MAP

2.1. **Properties.** We introduce the **logistic map**:

$$x_{n+1} = rx_n(1 - x_n). \tag{2.1}$$

The logistic map is used to describe the constrained growth of a population in discrete time. The state $x_n \geq 0$ represents the size of the population at time n, and $r \geq 0$ is a parameter that controls the growth rate. Plotting x_{n+1} vs x_n on the interval $x \in [0, 1]$ (see Figure 5) gives us that the map achieves a maximum at $r/4$.

Since we want to analyze the behavior of fixed points in the map, we restrict r to $0 \leq r \leq 4$ so that the logistic map maps $[0, 1]$ to itself. We want to know how the behavior of the map changes as we change r. Using cobwebbing (see Figure 6), we see that for all $0 \leq r < 1$,

$$\lim_{n\to\infty} x_n = 0. \tag{2.2}$$

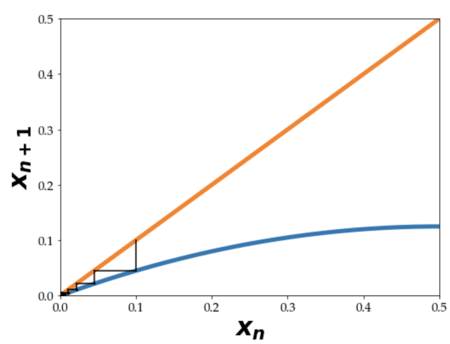

FIGURE 6. Cobweb when $r = 1/2$.

For a fixed $1 \leq r < 3$, we plot x_n vs n to see the behavior of the map (2.1). The plot for $r = 2.8$ is shown in Figure 7a. We see that eventually x_n converges to a fixed point, and the population stays at this size.

However, as we increase r beyond this range, we see an interesting change in behavior. In Figure 7b, we see that the population is constantly alternating between a large population size and a smaller population size (periodic points). Since x_n repeats every other iteration, this orbit has period two.

In Figure 7c, we see that x_n repeats every four iterations, giving it period four. In fact, the values of r_n, where r_n is the value of r when a period-2^n orbit first appears, has been experimentally computed, and the difference between successive r_n decreases by a factor of

$$\lim_{n\to\infty} \frac{r_n - r_{n-1}}{r_{n+1} - r_n} = 4.669\ldots. \tag{2.3}$$

Thus, we see a geometric convergence and find that $r_n \to r_\infty \approx 3.57$.

This raises the question, what happens for $r > r_\infty$? Looking at the time series in Figure 7d and cobweb in Figure 8 for $r = 3.9$, we see very complex behavior with no clear pattern. To better see how the behavior of the system changes as we alter r, we plot what is called an orbit diagram in Figure 9. The graph plots the attractors as a function of r. The picture is similar to a bifurcation diagram, except we only show the attracting points.

Now, we can graphically see the period-doubling bifurcation shown by the splitting of the branches, which represents the periodic orbits doubling in period. We also see that after $r_\infty \approx 3.57$, the map becomes chaotic and we now have infinitely many attractors.

2.2. **Analysis.** We show analytically some of the interesting behavior the logistic map displays.

2.2.1. *Stability.* First, we find all the fixed points and determine their stability. We solve for the roots of

$$x_f = f(x_f) = rx_f(1 - x_f), \tag{2.4}$$

and so we examine

$$x_f - rx_f(1 - x_f) = x_f(1 - r(1 - x_f)) = 0. \tag{2.5}$$

This implies fixed points

$$x_f = 0 \qquad \text{for } 0 \leq r \leq 4, \tag{2.6}$$

$$x_f = 1 - 1/r \quad \text{for } 1 \leq r \leq 4. \tag{2.7}$$

The range of r where the roots of (2.5) are fixed points comes from the fact that our domain and range is $[0, 1]$.

To determine their stability, we look at the derivative

$$f'(x_f) = r - 2rx_f. \tag{2.8}$$

The zero state is stable for $r < 1$ and unstable for $r > 1$ since

$$f'(0) = r. \tag{2.9}$$

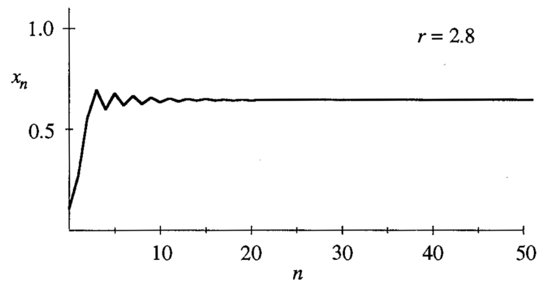

(A) The graph converges to a single population size.

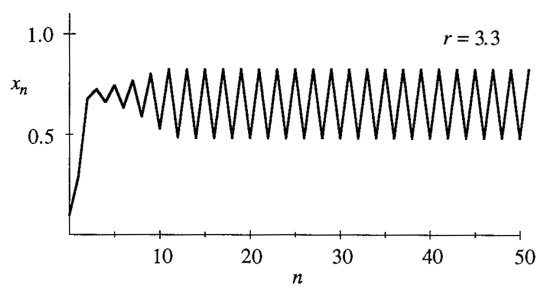

(B) The graph oscillates between two population sizes.

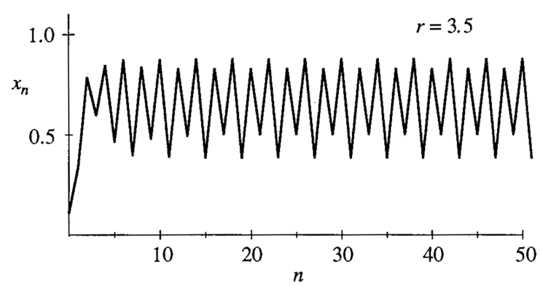

(C) The graph oscillates between four population sizes.

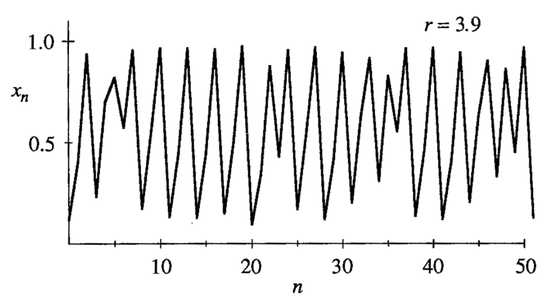

(D) Aperiodic points.

FIGURE 7. Plotting x_n vs n for various values of r. The discrete points are connected with lines to make it easier to read. Reprinted from [1], p.354-355.

This makes sense with our previous analysis that the cobweb goes to zero for $r < 1$. We also know that the state $1 - 1/r$ is stable for $1 < r < 3$ and unstable for $r > 3$, since

$$f'\left(1 - \frac{1}{r}\right) = r - 2r\left(1 - \frac{1}{r}\right) = 2 - r. \tag{2.10}$$

Thus, we can see this as a transcritical bifurcation at $r = 1$ when the zero state becomes unstable and the state $1 - 1/r$ becomes stable.

2.2.2. *Period doubling.* Next, we show that for $r > 3$, the logistic map has a period-two trajectory. To do this, we find points p, q such that

$$f(p) = q, \quad f(q) = p, \tag{2.11}$$

and

$$f^2(p) = p, \quad f^2(q) = q, \tag{2.12}$$

(periodic points with period two).

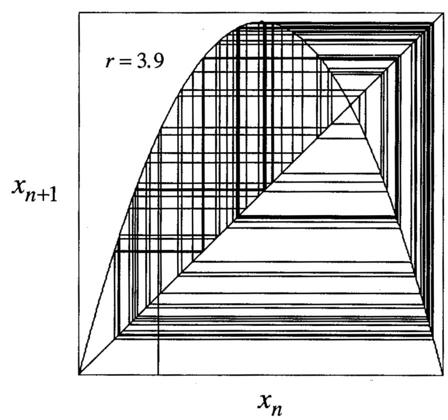

FIGURE 8. The cobweb never settles down on some point(s). Reprinted from [1], p.356.

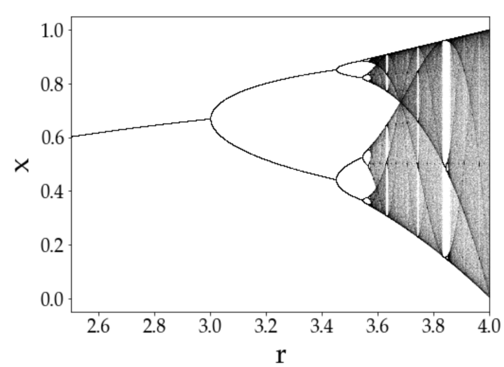

FIGURE 9. The orbit diagram of the logistic map

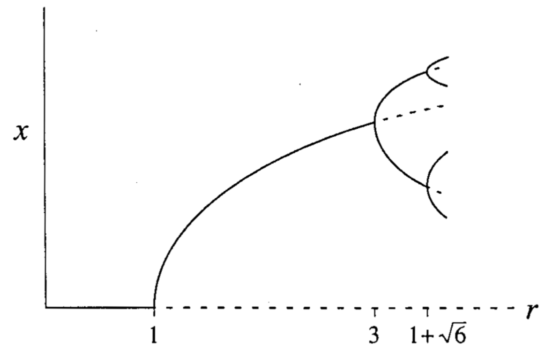

FIGURE 10. A partial bifurcation diagram of the logistic map. Reprinted from [1], p.361.

While $f^2(x)$ is a quartic polynomial and we need to solve $f^2(x) = x$, we recognize that we already have two trivial solutions, zero and $1 - 1/r$, since if they are fixed points, $f(f(x_f)) = f(x_f) = x_f$. We want to solve:

$$f^2(x) - x = r^2 x(1-x)[1 - rx(1-x)] - x = 0. \tag{2.13}$$

We remove the factors x and $x-(1-\frac{1}{r})$ through long division and use the quadratic equation to get the roots

$$p, q = \frac{r + 1 \pm \sqrt{(r-3)(r+1)}}{2r}. \tag{2.14}$$

From this, we can tell that we have a period-two trajectory for $r > 3$ since both roots are real in that range. In particular, we note that at $r = 3$, both roots are equal to $x = 1 - 1/r = 2/3$, which shows that the periodic trajectory emerges continuously from the previous stable trajectory.

2.2.3. *Stability of periodic orbits.* Finally, we want to look at the stability of the period-two trajectory. We want to show that it is attracting for

$$3 < r < 1 + \sqrt(6), \tag{2.15}$$

which is exactly the r before a period-four trajectory emerges. To determine stability, we find the derivative of f^2:

$$\begin{aligned} \lambda &= \frac{d}{dx}(f(f(x))\bigg|_{x=p} \\ &= f'(f(p))f'(p) \\ &= f'(q)f'(p). \end{aligned} \tag{2.16}$$

Note that we get the same λ for states p and q, proving that they bifurcate at the same time. For their stability, we examine

$$\lambda = r(1-2q)r(1-2p) = r^2[1 - 2(p+q) + 4pq]. \tag{2.17}$$

Substituting (2.14) into the above expression gives us

$$\lambda = r^2 \left[1 - 2\left(\frac{r+1}{r}\right) + 4\left(\frac{r+1}{r^2}\right)\right] = 4 + 2r - r^2. \tag{2.18}$$

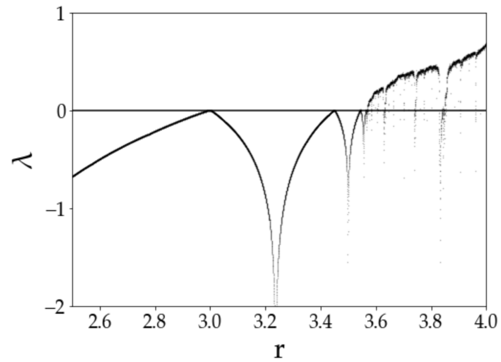

FIGURE 11. We see that around the r-value where the logistic map becomes chaotic, the Liapunov exponent becomes positive

We want $|\lambda| < 1$ for the orbit to be stable, and so (2.15) is sufficient. We also see this in a bifurcation diagram, Figure 10, that includes both the stable and unstable branches of the logistic map.

2.3. **Liapunov Exponent.** For certain values of r, we see the existence of aperiodic orbits. However, are these orbits truly "chaotic"? We will define chaos rigorously in the next section. For now, we note that one of the characteristics of chaotic systems is that they display **sensitive dependence on initial conditions**, where nearby orbits will, on average, move away at an exponential rate.

For an initial condition x_0, consider a close state $x_0 + \delta_0$, where δ_0 is small. Define δ_n to be the separation between the orbits after n iterations. If

$$|\delta_n| \approx |\delta_0| e^{n\lambda}, \tag{2.19}$$

we call λ the **Liapunov exponent**. A positive Liapunov exponent is an indicator that the system may be chaotic.

We can derive an explicit formula. From (2.19), we know $\log|\delta_n| \approx n\lambda \log|\delta_0|$, and so

$$\lambda \approx \frac{1}{n} \log\left|\frac{\delta_n}{\delta_0}\right|. \tag{2.20}$$

Notice that $\delta_n = f^n(x_0 + \delta_0) - f^n(x_0)$, hence the right hand side of (2.20) is exactly

$$\frac{1}{n} \log\left|\frac{f^n(x_0 + \delta_0) - f^n(x_0)}{\delta_0}\right|. \tag{2.21}$$

Taking $\delta_0 \to 0$, the above becomes the derivative

$$\frac{1}{n} \log\left|(f^n)'(x_0)\right|. \tag{2.22}$$

Using chain rule:

$$\log\left|\prod_{i=0}^{n-1} f'(x_i)\right| = \sum_{i=0}^{n-1} \log|f'(x_i)|. \tag{2.23}$$

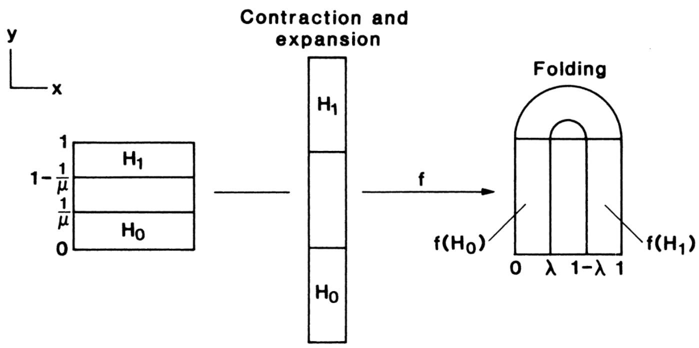

FIGURE 12. Reprinted from [2], p.556.

If the limit exists, then we define the Liapunov exponent as

$$\lambda \equiv \lim_{n\to\infty}\left(\frac{1}{n}\sum_{i=0}^{n-1}\ln|f'(x_i)|\right). \tag{2.24}$$

While the Liapunov exponent depends on the initial conditions, it has the same value for all initial conditions within a basin of attraction of an attractor (since in the limit all the orbits will converge to the attractor). For stable fixed points and periodic orbits, $\lambda < 0$, while for "chaotic attractors," $\lambda > 0$. For the logistic map, we can numerically compute λ and plot it as a function of r, see Figure 11.

3. Chaos

3.1. **Smale Horseshoe.** To be able to define precisely what chaos is, we turn to the simplest map that exhibits chaotic behavior to narrow down the essential properties of chaos, the Smale Horseshoe map. The **Smale Horseshoe map** is a two-dimensional map $f : D \to D$, where D is a square in $\mathbb{R}^2$:

$$D \equiv \{(x,y) \in \mathbb{R}^2 \mid x, y \in [0,1]\}. \tag{3.1}$$

Roughly, f contracts D in the x-direction, extends the y-direction, and then folds D back on itself. The backward iteration of f, f^{-1} contracts D in the y-direction, extends the x-direction, and then folds D back on itself. Figure 12 illustrates this.

More explicitly, for some fixed parameters $\mu^{-1} > 0$ and $\lambda < 1/2$, we map

$$H_0 = \{(x,y) \in D \mid y \in [0, \mu^{-1}]\}, \tag{3.2}$$

$$H_1 = \{(x,y) \in D \mid y \in [1-\mu^{-1}, 1]\}, \tag{3.3}$$

to

$$f(H_0) = \{(x,y) \in D \mid x \in [0,\lambda]\} \qquad \equiv V_0, \tag{3.4}$$

$$f(H_1) = \{(x,y) \in D \mid x \in [1-\lambda, 1]\} \equiv V_1. \tag{3.5}$$

Essentially, the horizontal rectangles H_0, H_1 are mapped to vertical rectangles V_0, V_1 respectively. The horizontal boundaries of H_0, H_1 are mapped to the horizontal boundaries of V_0, V_1 respectively (likewise for vertical boundaries). In the opposite direction, f^{-1} maps V_k and their boundaries to H_k and their boundaries.

Now, we introduce two important observations.

Properties 3.6. For the Smale Horshoe map f given above, we have the following:

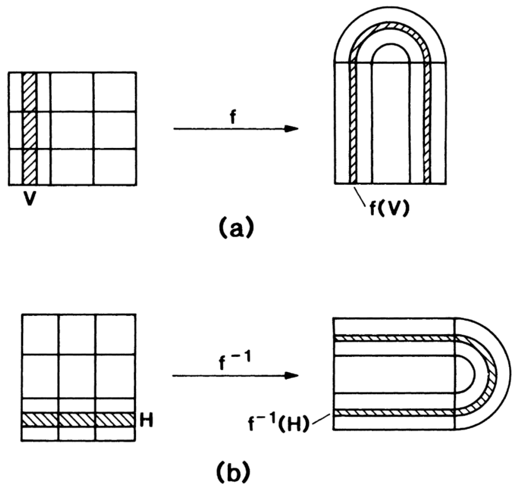

FIGURE 13. What happens to a rectangle in the square through a mapping. Reprinted from [2], p.558.

(1) If V is a vertical rectangle in D, then $f(V) \cap D$ contains exactly two vertical rectangles, one in V_0 and one in V_1, each with width λ times that of V.
(2) If H is a horizontal rectangle in D, then $f^{-1}(H) \cap D$ contains exactly two horizontal rectangles, one in H_0 and one in H_1, each with width μ times that of H.

See Figure 13 for a visualization. The proof uses the definition of f. The vertical rectangle V intersects the horizontal boundaries of both H_0 and H_1, so when we map those pieces of boundaries to the horizontal boundaries of V_1, V_2, the image $f(V)$ would appear in both V_0 and V_1, creating two vertical rectangles. The width contracts by λ because of the contraction in the x-direction of H_0 and H_1 via (3.4) and (3.5). Property 2 for a horizontal rectangle H follows similarly.

Now, we want to look at the invariant set Λ of the map. We think of the invariant set as a set of points that remain in D after all forward and backward iterations of the map (f and f^{-1}). Thus,

$$\Lambda = \bigcap_{n=-\infty}^{\infty} f^n(D). \tag{3.7}$$

We first focus on constructing $\bigcap_{n=0}^{k} f^n(D)$ and take $k \to \infty$. Then, the negative portion will follow analogously. We know that V_0 and V_1 are in the first intersection, $D \cap f(D)$. To find what remains in

$$D \cap f(D) \cap f^2(D), \tag{3.8}$$

we use the first property on V_0 and V_1. By Property 1, since V_0 and V_1 intersects H_0 and H_1 and so does their horizontal boundaries, then (3.8) will contain exactly four vertical rectangles: two in V_0 and two in V_1. The map f contracts width by a factor of λ, so the width of the rectangles in (3.8) is λ^2. Doing the same thing for

$$D \cap f(D) \cap f^2(D) \cap f^3(D), \tag{3.9}$$

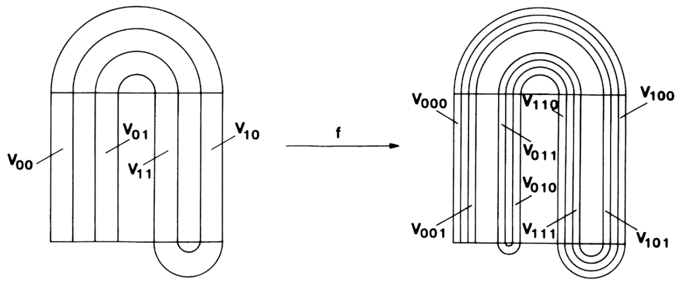

FIGURE 14. Drawing (3.8) and (3.9). Reprinted from [2], p.561.

we get eight vertical rectangles (V_0 and V_1 each have four, each rectangle of (3.8) has two), all having width λ^3. Pictorially, the construction looks like Figure 14.

We see that $\bigcap_{n=0}^{k} f^n(D)$ will contain 2^k vertical rectangles, each of width λ^k. We observe there is a unique k-length binary sequence that labels each rectangle. Then, taking $k \to \infty$ and using the fact that a decreasing intersection of compact sets (rectangles are closed and bounded) is non-empty, we see that

$$\bigcap_{n=0}^{\infty} f^n(D) \tag{3.10}$$

consist of infinitely many vertical rectangles with zero width ($\lim_{k\to\infty} \lambda^k = 0$). In the limit, we have recovered a set of vertical lines that we may uniquely label with an infinite sequence of zeros and ones. Doing the same for

$$\bigcap_{n=0}^{-\infty} f^n(D) \tag{3.11}$$

again yields infinitely many horizontal lines uniquely labeled by an infinite sequence of zeros and ones.

Then, Λ, which is the intersection of the sets (3.10) and (3.11), consists of infinitely many points since the vertical and horizontal lines from each set intersect at a unique point in D. Additionally, any $p \in \Lambda$, formed from the intersection of a vertical line $V_{s_{-1},\ldots,s_{-k},\ldots}$ in (3.10) labeled $s_{-1}, \ldots, s_{-k}, \ldots$ and a horizontal line $H_{s_0,\ldots,s_k,\ldots}$ in (3.11) labeled $s_0, \ldots, s_k, \ldots$, can be uniquely labeled with a bi-infinite sequence

$$\ldots, s_{-k}, \ldots s_{-1}.s_0, \ldots, s_k, \ldots, \tag{3.12}$$

where the dot separates the forward and backward iterations. Under such a labeling of the vertical and horizontal rectangles, we can find the associated sequence of $f^k(p)$ by shifting the dot in the label p by k places (left if $k < 0$, right if $k > 0$). To understand this more, we turn to symbolic dynamics.

3.2. **Symbolic Dynamics.** Let Σ be the space of bi-infinite sequences of zeros and ones which will label the points in Λ. We say that two sequences are "close" if they agree on a long central block. We define the shift map $\sigma : \Sigma \to \Sigma$ that shifts the dot to the right by one place:

$$\sigma(\{\ldots, s_{-n}, \ldots, s_{-1}.s_0, s_1, \ldots, s_n, \ldots\}) = \{\ldots, s_{-n}, \ldots, s_{-1}, s_0.s_1, \ldots, s_n, \ldots\}. \tag{3.13}$$

Now, we look at the dynamics of σ, especially the orbits of points in Σ under the shift map. We note that there are only two fixed points: the sequence of all zeros and sequence of all ones. Periodic orbits are represented by repeating sections of finite length in the sequence, like $\{\overline{10}.\overline{10}\}$. We then see that the length of the repeating section is exactly the period of the orbit, because we need to move the decimal point over the entire section before we get the original sequence back:

$$\sigma(\{\overline{10}.\overline{10}\}) = \{\overline{01}.\overline{01}\}, \tag{3.14}$$

$$\sigma(\{\overline{01}.\overline{01}\}) = \{\overline{10}.\overline{10}\}, \tag{3.15}$$

$$\sigma^2(\{\overline{10}.\overline{10}\}) = \{\overline{10}.\overline{10}\}. \tag{3.16}$$

These repeating sections can have arbitrarily many symbols, but must be finite. Thus, σ has a countable number of periodic orbits of any period.

We also see that σ has uncountably many non-periodic orbits. We see this from the fact that we can associate any bi-infinite sequence to an infinite one:

$$..., s_{-n}, ..., s_{-1}.s_0, ..., s_n, ... \mapsto .s_0, s_1, s_{-1}, ..., s_n, s_{-n}, ... \tag{3.17}$$

We know that numbers in $[0, 1]$ can be expressed as binary expansions (the infinite sequences of zeros and ones), with the uncountably many irrationals corresponding to non-repeating sequences in Σ. The non-repeating sequences are the non-periodic orbits, so we have uncountably many non-periodic orbits.

Finally, we assert that σ has a dense orbit. We know these three facts about the shift map, and we can construct a homeomorphism $\phi : \Lambda \to \Sigma$. Thus, the Smale Horeshoe map f on D and the shift map σ on Σ are topologically conjugate, meaning the diagram in Figure 15 commutes.

$$\begin{tikzcd} \Lambda \arrow[r, "f"] \arrow[d, "\phi"'] & \Lambda \arrow[d, "\phi"] \\ \Sigma \arrow[r, "\sigma"] & \Sigma \end{tikzcd}$$

FIGURE 15. Reprinted from [2], p.572.

From this, we know that f has these properties of σ:

Properties 3.18. For the Smale Horshoe map, there exists

(1) countable periodic orbits of any period,
(2) uncountable non-periodic orbits,
(3) a dense orbit.

Additionally, we assert that Σ is uncountable, perfect, and totally disconnected, making it a **Cantor set**. These properties carry over to the invariant set, meaning Λ is a Cantor set. This invariant set is an attractor (since we can find orbits arbitrarily close to it) with fractal structure and measure zero, which we call a **strange attractors**. Strange attractors are typically associated with chaotic dynamics.

From Properties 3.18 , we see that the dynamics of f on Λ fulfills the properties of deterministic chaos. Generally, chaotic dynamical systems have

(1) sensitive dependence on initial conditions,

(2) **topologically transitivity**, meaning that for any two open sets of initial states, some iteration of one will intersect the other,
(3) dense periodic orbits.

Topologically transitivity follows from the existence of a dense orbit on a compact set. We need this property in addition to sensitive dependence on initial conditions, because a map which merely doubles the values of states has sensitive dependence but not chaos, as we can predict its behavior. We adopt the convention in [2] and call a dynamical system **chaotic** if it has sensitive dependence on a closed invariant set of more than one orbit.

For the Smale Horseshoe map, we will show sensitive dependence on initial conditions in Λ through symbolic dynamics. It is obvious that Λ is compact since it is closed and bounded. Consider some $p \in \Lambda$ represented by

$$\phi(p) = \{s_{-n}, ..., s_{-1}.s_0, ..., s_n, ...\}. \tag{3.19}$$

Take an ϵ-neighborhood around p and then we can find, for a finite $N = N(\epsilon)$, a point $x \in \Lambda$ which is represented by a sequence $\phi(x)$ that is identical to $\phi(p)$ up to the $(N+1)$th symbol.

Now, suppose the $(N+1)$th symbol of $\phi(p)$ is zero and $\phi(x)$ is one. This shows that after a finite number of iterations, no matter how small of a neighborhood we take, $f^N(p)$ would be in H_0 and $f^N(x)$ would be in H_1, which are separated by a distance of at least $1 - 2\lambda$. Thus, arbitrarily close initial conditions can evolve to become arbitrarily far apart (within the invariant set), but can also evolve to be arbitrarily close in the attractor, which is why their behavior appears to be random.

3.3. **Conley-Moser Conditions.** Before we state the Conley-Moser conditions for chaos, we must define several terms. Consider the unit square D with points labelled (x, y). A μ_v**-vertical curve** is a graph $v(y)$ of some function $v : [0, 1] \to [0, 1]$ such that

$$\max_{y_1, y_2 \in [0,1]} \frac{|v(y_1) - v(y_2)|}{|y_1 - y_2|} \leq \mu_v. \tag{3.20}$$

A μ_h**-horizontal curve** is defined analogously, but for some $h(x)$ and μ_h.

A μ_v**-vertical strip** is the set

$$V = \{(x, y) \in D \mid x \in [v_1(y), v_2(y)]\} \tag{3.21}$$

given by two μ_v-vertical curves $v_1(y), v_2(y)$ which do not intersect. The width $d(V)$ of a vertical strip $V \subset D$ is

$$d(V) = \max_{y \in [0,1]} |v_2(y) - v_1(y)|. \tag{3.22}$$

Again, we define a μ_h**-horizontal strip** and its width analogously. We assert these two lemmas about the curves and strips:

Lemma 3.23. *If $V_1 \supset V_2 \supset ...V_k \supset ...$ is a nested sequence of μ_v-vertical strips such that $\lim_{k\to\infty} d(V_k) = 0$, then*

$$V_\infty \equiv \bigcap_{k=1}^{\infty} V_k$$

is a μ_v-vertical curve. The analogous holds for horizontal strips and curves.

Lemma 3.24. *If $0 \leq \mu_v \mu_h < 1$, then a μ_v-vertical curve and a μ_h-horizontal curve intersect at a unique point.*

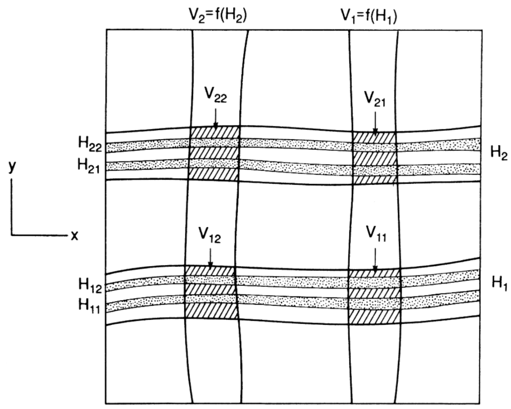

FIGURE 16. Naming of the strips. Reprinted from [2], p.603.

Let $S = \{1, 2, ..., n\}$ be an index set with at least two elements. For $i = 1, 2, ..., n$, denote H_i as a set of disjoint μ_h-horizontal strips and V_i a set of disjoint μ_v-vertical strips. Consider a map $f : D \to \mathbb{R}^2$, where D is the unit square. We can prove using the above lemmas that if f satisfies two conditions, then f has an invariant Cantor set $\Lambda \subset D$ that is topologically conjugate to a full shift on n symbols, Σ^n. These conditions are called the **Conley-Moser conditions**, and the invariant set will have chaotic dynamics.

Definition 3.25. The Conley-Moser conditions are:

(1) If $0 \leq \mu_h \mu_v < 1$, then $f(H_i) = V_i$ for $i = 1, 2, ..., n$, where the horizontal boundaries of H_i map to the horizontal boundaries of V_i and the vertical boundaries of H_i map to the vertical boundaries (homeomorphic mapping).

(2) Define H_i' as $f^{-1}(H) \cap H_i$, where H is a μ_h-horizontal strip in $\bigcup_{i \in S} H_i$. We require that H_i' is a μ_h-horizontal strip for all $i \in S$ and

$$d(H_i') \leq x_h d(H)$$

for some $0 < x_h < 1$. This must also hold for vertical strips, and the condition is defined analogously, with $V_i' \equiv f(V) \cap V_i$.

These two conditions show that geometrically, chaos arises from some form of "stretching" and "squishing" of the square and folding it back onto itself.

Theorem 3.26 ([2], p.590)**.** *If f satisfies Conditions 1 and 2, then f has an invariant Cantor set Λ on which it is topologically conjugate to a full shift on n symbols.*

While the first condition is straightforward, it can be difficult to directly verify the second condition. Since the second condition deals with the rate of expansion and contraction, we want to find an equivalent condition by looking at the derivatives of maps. Let $V_{ji} \equiv f(H_i) \cap H_j$ and

$$H_{ij} \equiv H_i \cap f^{-1}(H_j) = f^{-1}(V_{ji}) \tag{3.27}$$

for $i, j \in S$, where S is the index set defined previously. Let H be the union of all such H_{ij} and V the union of V_{ji}, and we see that $f(H) = V$. Figure 16 depicts the case where $n = 2$.

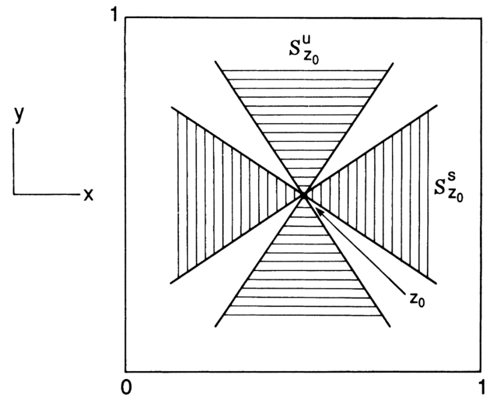

FIGURE 17. Sectors. Reprinted from [2], p.604.

We require that f is C^1 and maps H diffeomorphically onto V. Let $(\xi_{z_0}, \eta_{z_0}) \in \mathbb{R}^2$ be a vector originating from point $z_0 = (x_0, y_0) \in H \cup V$. We define the **stable sector at** z_0 as

$$S^s_{z_0} = \{(\xi_{z_0}, \eta_{z_0}) \in D : |\eta_{z_0}| \le \mu_h |\xi_{z_0}|\}. \tag{3.28}$$

The **unstable sector at** z_0 is

$$S^u_{z_0} = \{(\xi_{z_0}, \eta_{z_0}) \in D : |\xi_{z_0}| \le \mu_v |\eta_{z_0}|\}. \tag{3.29}$$

Geometrically, the stable sector can be seen as a "cone" of vectors originating from z_0, where each vector has a maximum absolute value slope of μ_h with respects to the x-axis. The unstable sector is the same, except each vector has a maximum absolute value slope of μ_v with respects to the y-axis. See Figure 17 for an illustration.

Now, we will define the **sector bundles**, which are unions of stable/unstable sectors over points in either H or V:

$$S^s_H = \bigcup_{z_0 \in H} S^s_{z_0} : \text{ stable sector bundle over } H, \tag{3.30}$$

$$S^u_H = \bigcup_{z_0 \in V} S^u_{z_0} : \text{ unstable sector bundle over } H, \tag{3.31}$$

$$S^s_V = \bigcup_{z_0 \in H} S^s_{z_0} : \text{ stable sector bundle over } V, \tag{3.32}$$

$$S^u_V = \bigcup_{z_0 \in V} S^u_{z_0} : \text{ unstable sector bundle over } V. \tag{3.33}$$

Then, we can give our alternative to the second Conley-Moser condition:

Definition 3.34.

(3) For the sector bundles defined above, we require

$$Df(S^u_H) \subset S^u_V \text{ and } Df^{-1}(S^s_V) \subset S^s_H.$$

In this alternate condition, $Df(S^u_H) \subset S^u_V$ means that for every $z_0 \in H$,

$$(\xi_{z_0}, \eta_{z_0}) \in S^u_{z_0} \Rightarrow Df(z_0)(\xi_{z_0}, \eta_{z_0}) \equiv \big(\xi_{f(z_0)}, \eta_{f(z_0)}\big) \in S^u_{f(z_0)}. \tag{3.35}$$

The statement $Df^{-1}(S^s_V) \subset S^s_H$ is defined similarly. In particular, we note that if $(\xi_{z_0}, \eta_{z_0}) \in S^u_{z_0}$ and $\xi_{f(z_0)}, \eta_{f(z_0)}) \in S^u_{f(z_0)}$, then

$$|\eta_{f(z_0)}| \geq \frac{1}{\mu}|\eta_{z_0}| \quad \text{for } 0 < \mu < 1 - \mu_h\mu_v. \tag{3.36}$$

Analogously, if $(\xi_{z_0}, \eta_{z_0}) \in S^s_{z_0}$ and

$$Df^{-1}(z_0)(\xi_{z_0}, \eta_{z_0}) \equiv (\xi_{f^{-1}(z_0)}, \eta_{f^{-1}(z_0)}) \in S^s_{f^{-1}(z_0)}, \tag{3.37}$$

then

$$|\xi_{f^{-1}(z_0)}| \geq \frac{1}{\mu}|\xi_{z_0}| \quad \text{for } 0 < \mu < 1 - \mu_h\mu_v. \tag{3.38}$$

Finally, we can state our theorem regarding sector bundles.

Theorem 3.39 ([2], p.605)**.** *If Conditions 1 and 3 hold with $0 < \mu < 1 - \mu_h\mu_v$, then Condition 2 holds with $x_h = x_v = \mu/(1 - \mu_h\mu_v)$.*

Thus, we can show chaos with either Conditions 1 and 2, or Conditions 1 and 3.

4. Hénon Map

To close off the paper, we want to prove that the **Hénon map**, which is a two-dimensional analog of the logistic map, is chaotic. The Hénon map F is given by the equations:

$$F : \begin{cases} x_{n+1} = a - by_n - x_n^2 \\ y_{n+1} = x_n \end{cases}. \tag{4.1}$$

There are critical values of a and b such that F exhibits chaos; that is F fulfills the properties of deterministic chaos. Here, we fix b and examine

$$B = \frac{(5 + 2\sqrt{5})(1 + |b|)^2}{4}. \tag{4.2}$$

Theorem 4.3 ([3])**.** *Let Λ be the invariant set of F. For $a > B$, Λ has a hyperbolic structure and is conjugate to the 2-shift.*

Proposition 4.4 ([2], p.610)**.** *For $a > B$, F satisfies Conley-Moser Condition 1.*

Proof. Let R be the larger root of

$$\rho^2 - (|b| + 1)\rho - a = 0, \tag{4.5}$$

and $S \subset \mathbb{R}^2$ the square with the center at the origin and vertices at $(\pm R, \pm R)$. We will show that for $a > B$, the condition

$$|x| \geq \lambda\frac{1 + |b|}{2} \tag{4.6}$$

divides S into two vertical strips and

$$|y| \geq \lambda\frac{1 + |b|}{2} \tag{4.7}$$

divides S into two horizontal strips that satisfy Condition 1.

For $x_0 = x$, we want to show that under F, the image of x_0 is in the horizontal strips specified by (4.7). Under F, we have that x_0 satisfies (4.6) and $y_1 = x_0$.

Thus, y_1 satisfies (4.7) such that the y-coordinates of the horizontal strip fulfill our requirements. For the x-coordinates,

$$x_1 = a - by_0 - x_0^2, \tag{4.8}$$

which implies that

$$x_1 \le a - by_0 - \left(\lambda \frac{1+|b|}{2}\right)^2. \tag{4.9}$$

Solving this yields that $|x_1| \le R$.

For the horizontal strips mapping to vertical strips $y_0 = y$, we do the same thing, except we have to use the inverse map, which can be found by solving for x_n and y_n and changing the index:

$$F^{-1} : \begin{cases} x_{n-1} = y_n \\ y_{n-1} = \dfrac{-x_n + a - y_n^2}{b} \end{cases}, \tag{4.10}$$

where x_{n-1}, y_{n-1} denotes the inverse iterations. Then, we see that $x_{-1} = y_0$, thus x_{-1} satisfies (4.6). For the y-coordinates, we have

$$y_{-1} = \frac{-x_0 + a - y_0^2}{b}, \tag{4.11}$$

as desired. □

Proposition 4.12 ([2], p.611)**.** *For $a > B$, F satisfies Conley-Moser Condition 3.*

Proof. Now, we will look at the sectors

$$S_\lambda^u = \{(\xi, \eta) \in S : |\xi| \ge \lambda|\eta|\}, \tag{4.13}$$

$$S_\lambda^s = \{(\xi, \eta) \in S : |\eta| \ge \lambda|\xi|\}. \tag{4.14}$$

If the inequality for a from before holds, we want to show that we can find $\lambda > 2$ so that S_λ^u is invariant under $DF(x, y)$ in the vertical strips and S_λ^s is invariant under $DF^{-1}(x, y)$ in the horizontal strips, thus satisfying Condition 3.

To show this, we first notice that the matrix of partial derivatives of the maps F and F^{-1} is

$$DF = \begin{pmatrix} -2x & -b \\ 1 & 0 \end{pmatrix} \tag{4.15}$$

and

$$DF^{-1} = \frac{1}{b}\begin{pmatrix} 0 & b \\ -1 & -2x \end{pmatrix}. \tag{4.16}$$

Since x satisfies (4.6), we have $2|x| \ge \lambda + \lambda|b|$. This implies that

$$2|x| - \frac{|b|}{\lambda} > 2|x| - \lambda|b| \ge \lambda \quad \text{and} \quad 2|x| - \lambda \ge \lambda|b|. \tag{4.17}$$

Now, consider a vector $(\xi_0, \eta_0) \in S_\lambda^u$ and $(\xi_1, \eta_1) = DF_x(\xi_0, \eta_0)$. Using DF_x, the reverse triangle inequality, the definition of unstable bundle ($|\eta_z| \ge \lambda|\xi_z|$), and the first inequality in (4.17), we see that

$$\begin{aligned} |\xi_1| &= |-2x\xi_0 + -B\eta_0| \ge 2|x||\xi_0| - |B||\eta_0| \\ &\ge \left(2|x| - \frac{|B|}{\lambda}\right)|\xi_0| \\ &\ge \lambda|\xi_0|. \end{aligned} \tag{4.18}$$

Similarly, using DF^{-1} and the second inequality in (4.17), we show that

$$
\begin{aligned}
|\eta_{-1}| &= \frac{|\xi_0 + 2x\eta_0|}{|b|} \\
&\geq \frac{(2|x| - \lambda)|\eta_0|}{|b|} \\
&\geq \lambda|\eta_0|.
\end{aligned} \tag{4.19}
$$

If the points (x_0, y_0) and $(x_1, y_1) = F(x_0, y_0)$ both satisfy (4.6), for $\lambda > 2$, then S^u_λ is invariant under $DF(x, y)$ (and $(\xi_1, \eta_1) \geq \lambda|\xi_0, \eta_0|$) and S^s_λ is invariant under $DF^{-1}(x, y)$ (and $\lambda(\xi_1, \eta_1) \leq |\xi_0, \eta_0|$).

Consider $(\xi_0, \eta_0) \in S^u_\lambda$ and $(\xi_1, \eta_1) = DF_{x_0}(\xi_0, \eta_0)$, noting that $\eta_1 = \xi_0$. Using that $|\xi_1| > \lambda|\xi_0|$, we find that

$$\lambda|\eta_1| = \lambda|\xi_0| \leq |\xi_1|, \tag{4.20}$$

which shows that $(\xi_1, \eta_1) \in S^u_\lambda$. Using the definition of S^u_λ, we see that

$$\lambda|\eta_0| \leq |\xi_0| = |\eta_1|, \tag{4.21}$$

proving the first part of the claim. The second part follows symmetrically. □

Proof of Theorem 4.3. With Propositions 4.4 and 4.12, we apply Theorem 3.39. We observe Theorem 3.26, and we are done. □

Acknowledgments

It is my pleasure to thank my mentor Hezekiah Grayer II for his help in guiding me through the material.

References

[1] Strogatz, Steven H. *Nonlinear dynamics and chaos with student solutions manual: With applications to physics, biology, chemistry, and engineering.* CRC press, 2018.

[2] Wiggins, Stephen. *Introduction to applied nonlinear dynamical systems and chaos.* Vol. 2. New York: springer-verlag, 1990.

[3] Devaney, Robert, and Zbigniew Nitecki. "Shift automorphisms in the Hénon mapping." *Communications in Mathematical Physics* 67, no. 2 (1979): 137-146.